Current Biology 16, 1337–1343, July 11, 2006 ©2006 Elsevier Ltd All rights reserved DOI 10.1016/j.cub.2006.06.030

Report

CKIε/*discs overgrown* Promotes Both Wnt-Fz/β-Catenin and Fz/PCP Signaling in *Drosophila*

Thomas J. Klein,[1] Andreas Jenny,[1] Alexandre Djiane,[1] and Marek Mlodzik[1,*]
[1] Department of Molecular, Cell, and Developmental Biology
Mount Sinai School of Medicine
1 Gustave L. Levy Place
New York, New York 10029

Summary

The related Wnt-Frizzled(Fz)/β-catenin and Fz/planar cell polarity (PCP) pathways are essential for the regulation of numerous developmental processes and are deregulated in many human diseases. Both pathways require members of the Dishevelled (Dsh or Dvl) family of cytoplasmic factors for signal transduction downstream of the Fz receptors. Dsh family members have been studied extensively, but their activation and regulation remains largely unknown. In particular, very little is known about how Dsh differentially signals to the two pathways. Recent work in cell culture has suggested that phosphorylation of Dsh by Casein Kinase I epsilon (CKIε) may act as a molecular "switch," promoting Wnt/β-catenin while inhibiting Fz/PCP signaling [1]. Here, we demonstrate in vivo in *Drosophila* through a series of loss-of-function and coexpression assays that CKIε acts positively for signaling in both pathways, rather than as a switch. Our data suggest that the kinase activity of CKIε is required for peak levels of Wnt/β-catenin signaling. In contrast, CKIε is a mandatory signaling factor in the Fz/PCP pathway, possibly through a kinase-independent mechanism. Furthermore, we have identified the primary kinase target residue of CKIε on Dsh. Thus, our data suggest that CKIε modulates Wnt/β-catenin and Fz/PCP signaling pathways via kinase-dependent and -independent mechanisms.

Results and Discussion

Dco/CKIε Functions in Wingless and PCP Signaling

Previous cell-culture assays had suggested that CKIε positively regulates Wnt-Fz/β-catenin signaling and that it antagonizes Fz/PCP signaling [1]. To confirm that CKIε is required for Wnt/β-catenin signaling in vivo, we examined loss of function (LOF) alleles of *discs overgrown* (*dco*/*doubletime*, the *Drosophila* CKIε gene) for phenotypes indicative of Wingless (Wg: *Drosophila* Wnt1) signaling defects. Consistent with previous data demonstrating a requirement for *dco* in disc growth [2], strong *dco*/*CKIε* alleles ($dco^{dbt\text{-}P}$) gave clones too small to analyze for disruption of Wg target-gene expression (not shown). We thus generated *dco*/*CKIε* mutant clones with the *Minute* technique (see Experimental Procedures). In these, expression of the Wg target gene *senseless* (*sens*) was lost in mutant cells (Figures 1A and 1A′). Accordingly, *dco*/*CKIε* adult wing clones show loss of margin bristles and/or parts of the wing margin (Figures 1B and 1C), consistent with a positive requirement for *dco* in Wg signaling. However, Wg targets that require lower levels of Wg signaling (e.g., *Dll*) were not affected (see Figure S1A in the Supplemental Data available online), indicating that *dco*/*CKIε* is only required for peak Wg signaling levels. Consistent with this finding, genome-wide RNAi screens for Wg signaling components identified *dco*/*CKIε* as a factor required for peak levels of β-catenin reporter expression [3].

The Fz/PCP pathway can easily be studied in *Drosophila*. The precise ommatidial arrangement in the eye and the orientation of hairs on the wing depend on correct Fz/PCP input. The two best-studied PCP signaling factors are Fz and Dsh, which also act in canonical Wnt/β-catenin signaling. To study the role of *dco*/*CKIε* in PCP, we first analyzed various heteroallelic *dco* combinations. In several of these (e.g., $dco^{dbt\text{-}P}/dco^{dbt\text{-}AR}$, Figure 1G), we observed typical PCP defects. Clones of a strong *dco*/*CKIε* allele show classical PCP phenotypes in the wing, with reoriented wing hairs (Figures 1D and 1E; *dco* PCP defects in the wing are autonomous, affecting only mutant cells, Figure 1D), and in the eye, with ommatidal chirality and orientation defects (Figure 1H; *dco*/*CKIε* clones also displayed ommatidia with photoreceptor loss, likely as a result of the cell viability requirement of Dco/CKIε [2]).

Our in vivo LOF analyses allow us to conclude that *dco*/CKIε is required for peak levels of Wg signaling, but does not appear to be a mandatory Wnt/β-catenin signaling component. In addition, our data identify *dco*/CKIε as a new factor required in Fz/PCP signaling.

Dco/CKIε Is Sufficient to Induce Wingless and PCP Signaling Phenotypes

To dissect the function of *dco*/*CKIε* in Wg and PCP signaling, we analyzed the effects of overexpressing CKIε. In the eye, we overexpressed *dco*/*CKIε* with *sevenless (sev)*-Gal4 (in R3/R4 cells that are critical for PCP establishment [4, 5]), which causes PCP phenotypes (Figure 1I; Table 1). In the wing, *decapentaplegic(dpp)*-Gal4-driven expression in a proximal-distal stripe along the A-P compartment boundary can be used to identify positive and negative effects on both Wg and PCP signaling [6]. *dpp*>CKIε displayed a mild but consistent PCP defect, a characteristic hair swirl near the intersection of the *dpp* stripe and wing margin. It also caused a small number of extra margin bristles, typical of increased Wg signaling (Figure 2D; Table S1).

Given that these phenotypes were mild, we sought to enhance them. Because CKIε requires an activating dephosphorylation event, which can be induced by Fz signaling [7], we next tested the effect of coexpressing CKIε with either Fz or Fz2 in the *dpp* stripe. Overexpression of Fz (*dpp*>Fz) causes a characteristic reorientation

*Correspondence: marek.mlodzik@mssm.edu

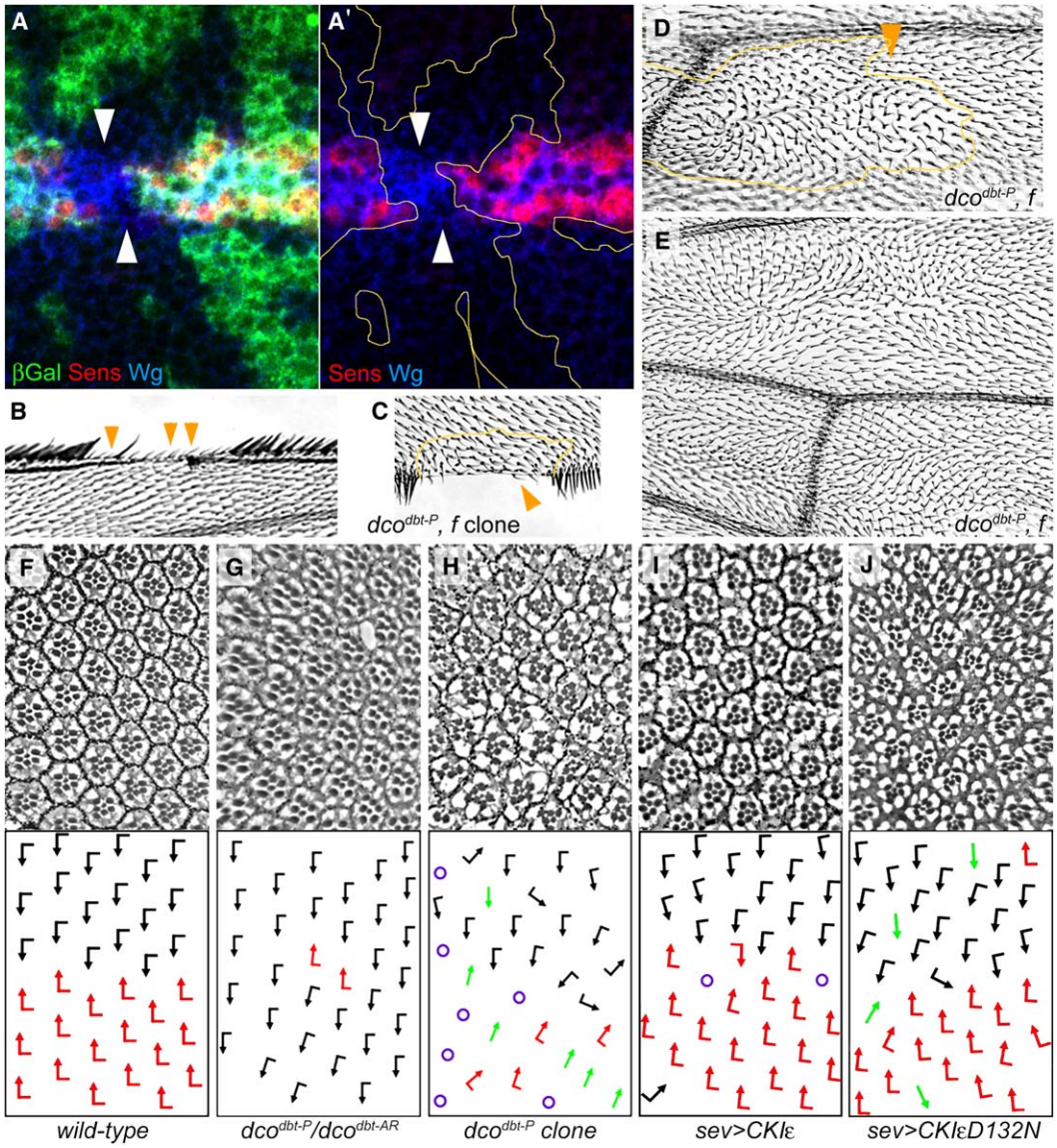

Figure 1. Dco/CKIε Regulates Both Wg and PCP Signaling in *Drosophila*

(A and A′) Confocal-microscopy image of a $dco^{dbt\text{-}P}$ mosaic third-larval-instar wing disc (mutant tissue is marked by absence of green staining; βgal). Anti-Sens staining (red) serves as a marker of Wg target-gene expression near wing margin; anti-Wg staining (blue) shows that Wg expression is not affected. Arrowheads in (A) and (A′) mark area with absence of Sens staining. Clones were generated with the *Minute* technique (see Experimental Procedures).

(B and C) $dco^{dbt\text{-}P}$ clones generated with standard (B) or *Minute* (C) techniques show loss of margin bristles in adult wing. Distal is to the right and anterior is up. Orange arrowheads point to areas with missing wing margin cells. The yellow line in (C) encircles a *forked* marked $dco^{dbt\text{-}P}$ clone, demonstrating that loss of margin bristles is autonomously associated with clonal tissue.

(D and E) $dco^{dbt\text{-}P}$ clones show autonomous planar cell polarity (PCP) wing hair defects (distal is right, anterior is up; yellow line in [D] outlines a larger *forked*-marked $dco^{dbt\text{-}P}$ clone). Note that distal to the outlined clone is a mosaic area where wild-type and mutant cells are mixed; none of the wild-type cells display a mutant phenotype (one example is highlighted by orange arrowhead). (E) shows a large *forked*-marked $dco^{dbt\text{-}P}$ clone demonstrating classical PCP defects.

(F–J) Tangential adult eye sections with corresponding schematics below each panel. Here and in all eye panels, red and black arrows represent the two chiral ommatidial forms, green arrows indicate symmetrical clusters, and purple circles ommatidia with a gain or loss of photoreceptors. All panels show an equatorial region, except (G), which shows a dorsal area. (F) *wild-type* eye. (G) $dco^{dbt\text{-}P}/dco^{dbt\text{-}AR}$ transheterozygous eye, showing mild PCP defects. (H) $dco^{dbt\text{-}P}$ *Minute* clonal eye, showing strong PCP defects and many unscorable ommatidia. (I) *sev*Gal4>UAS-CKIε, showing both PCP defects and unscorable ommatidia. (J) *sev*Gal4>UAS-CKIεD132N, showing stronger, clean PCP defects.

of wing hairs that point away from the expression domain (Figure 2B), but does not induce ectopic margin bristles. Strikingly, coexpression of Fz and CKIε leads to a dramatic synergy, with enhanced PCP defects and a large number of extra margin bristles in the expression domain (Figure 2C and Table S1), indicative of a positive CKIε role in both Wg and PCP signaling. Consistently, expression of Fz or CKIε alone is not sufficient to induce visible changes in Wg target-gene expression, but coexpression of CKIε and Fz cell-autonomously induces ectopic Senseless-positive cells (Figures S1B and S1C and data not shown).

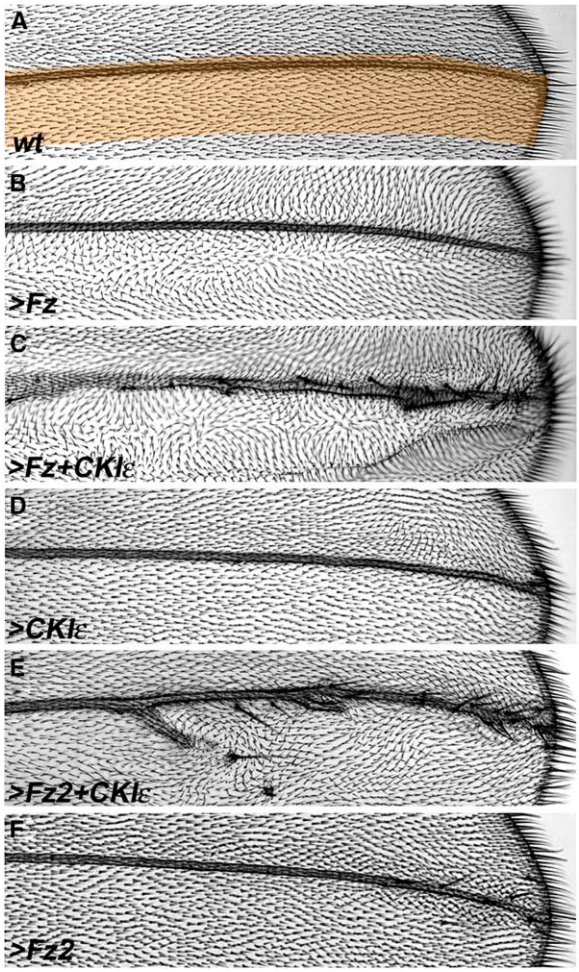

Figure 2. Dco/CKIε Acts Synergistically with Fz and Fz2 in *Drosophila* Wing Patterning

Anterior is up and distal is right in all panels.
(A) Wild-type wing (orange band highlights *dpp* expression domain).
(B) *dpp*Gal4>UAS-Fz wing (at 25ºC). Wing hairs point away from the *dpp* stripe, indicating a GOF PCP phenotype.
(C) *dpp*Gal4>UAS-Fz, UAS-CKIε wing (at 25ºC). Wing shows many extra margin bristles along the *dpp* stripe (mostly along wing vein), and wing hairs point away from the *dpp* stripe more dramatically than in (B), indicating an enhanced GOF PCP phenotype.
(D) *dpp*Gal4>UAS-CKIε wing (at 25ºC), showing a small wing-hair swirl near the intersection of the *dpp* stripe and wing margin and an ectopic margin bristle.
(E) *dpp*Gal4>UAS-Fz2, UAS-CKIε wing (at 18ºC; this combination is lethal at 25ºC), showing many extra margin bristles along the length of the *dpp* stripe as well as wing-hair swirls.
(F) *dpp*Gal4>UAS-Fz2 wing (at 18ºC), showing few ectopic margin bristles near the intersection of the *dpp* stripe and the margin. For quantification of all results, see Table S1.

dpp>Fz2 induces many ectopic margin bristles near the intersection of *dpp* expression and the wing margin (at 25ºC; Table S1). Because *dpp*-driven coexpression of Fz2 and CKIε at 25ºC is lethal, we examined the *dpp*>Fz2, CKIε coexpression in flies raised at 18ºC (allowing for weaker Gal4-driven expression; [8]). *dpp*>Fz2 at 18ºC induces only few margin bristles (Figure 2F; Table S1), a phenotype that is enhanced upon coexpression with CKIε (Figure 2E and Table S1; *dpp*>Fz2, CKIε coexpression also induces PCP-like hair swirls, although this effect could be indirect given that this combination induces wing-margin-like vein tissue, which could repolarize parts of the wing blade).

Taken together with the LOF analyses, these data demonstrate a positive, synergistic role for Dco/CKIε not only in Wg signaling, but also in Fz/PCP signaling.

Dco/CKIε Promotes Both Wg and PCP Signaling in the *Drosophila* Eye

To confirm that *dco*/*CKIε* acts positively for both pathways in vivo, we analyzed genetic interactions of *dco* with known Wg and PCP signaling factors in the eye (Figure 3 and Table 1). Overexpression of Fz (*sevFz*) causes strong PCP defects, a phenotype that is significantly suppressed by the removal of a single copy of *dco* (Figures 3A and 3B). Overexpression of Strabismus (Stbm; also known as Van Gogh or Vang), an antagonist of Fz/PCP signaling [9–11], with *sev*Gal4 (*sevStbm*) causes mild PCP defects, which are enhanced by removal of a copy of *dco* (Figures 3C and 3D), again supporting a positive role for *dco* in Fz/PCP signaling.

We next analyzed the effect of removing a copy of *dco* in the context of Dsh overexpression (*sev*>Dsh). *sev*>Dsh causes both PCP defects and loss of photoreceptors (Figure 3E), with the latter resembling the effect of *sev*>Wg [12]. Removing a copy of *dco* strongly suppresses the loss-of-photoreceptor phenotype, supporting a positive role for *dco* for peak Wg signaling (Figure 3F and Table 1). Assessing the effect of the removal of a copy of *dco* on the PCP in *sev*>Dsh is not possible, because the loss-of-photoreceptor phenotype masks PCP defects in many ommatidia.

In addition, we performed genetic analyses with overexpressed CKIε. *sev*>CKIε eyes exhibit mild PCP defects and a small percentage of ommatidia with a change in photoreceptor number (Figures 1I and 3G). Removal of a single copy of *dsh* suppressed the PCP and photoreceptor number defects, consistent with Dco/CKIε acting positively together with Dsh to elicit both phenotypes (Figure 3H and Table 1). Consistent with the coexpression results in the wing, these interactions support a positive role for *dco*/CKIε in both Wg and Fz/PCP signaling.

CKIε Phosphorylates Dsh at Serine 236 In Vitro

On the basis of the genetic interaction data with Dsh and cell-culture and in vitro kinase assays that have shown that CKIε can bind and phosphorylate Dsh [13–15], Dsh appears to be a likely phosphorylation target of CKIε. The actual site of phosphorylation on Dsh, however, has not been mapped. To narrow down the region of phosphorylation, we generated a series of GST-Dsh constructs covering all domains (Figure 4A). In vitro kinase assays using CKIε showed specific phosphorylation of all Dsh isoforms containing the basic region and PDZ domain (GST-Dsh, GST-bPDZ, GST-ΔC), but not of those containing just the PDZ (GST-PDZ) or other parts of Dsh (Figure 4B).

To determine the exact site of phosphorylation, we analyzed the region N terminal to the PDZ domain for conserved CKIε consensus sites [16, 17] and identified a likely motif (Figure 4C). In this motif, S236 is predicted to be the first serine residue phosphorylated by CKIε (green arrow; Figure 4C). When this serine is mutated to alanine (within GST-bPDZ), CKIε is no longer able to phosphorylate Dsh (Figure 4D). Interestingly, this residue

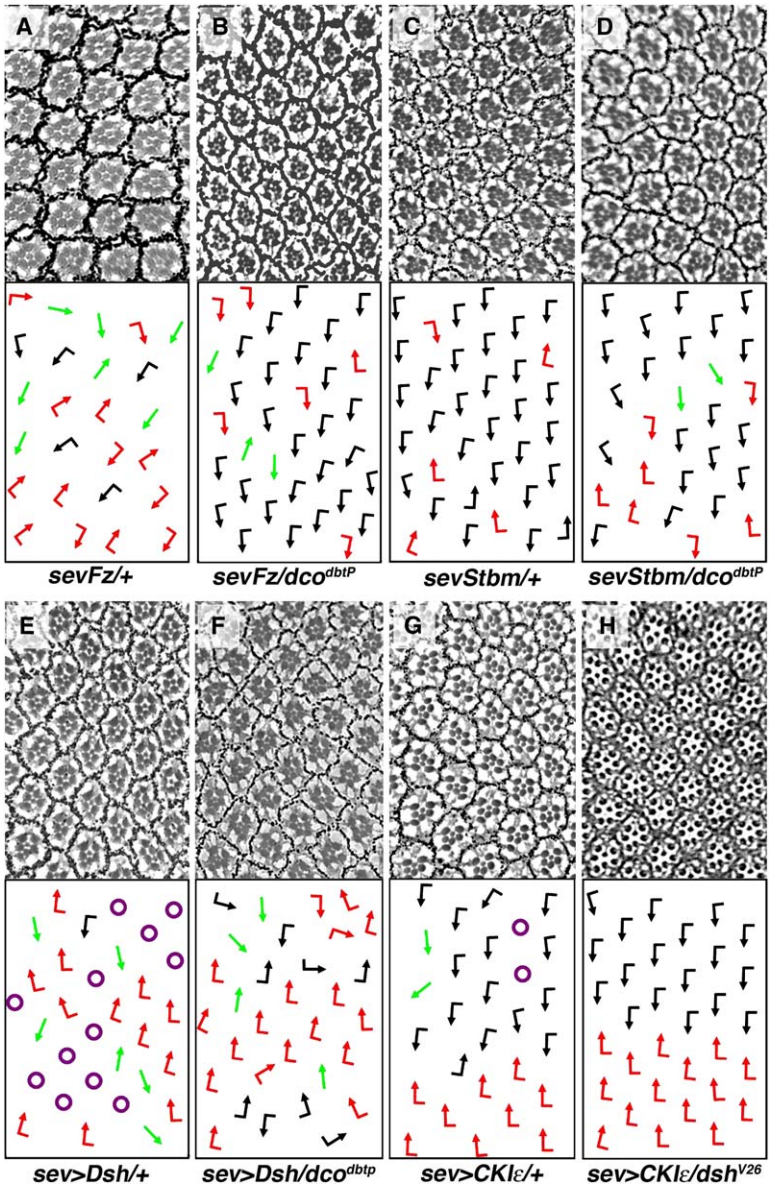

Figure 3. Dco/CKIε Acts Positively for Wg and Fz/PCP Signaling in the *Drosophila* Eye

All panels show tangential adult eye sections with the corresponding schematics and genotypes below. For quantification of results, see Table 1.

(A–D) *dco/CKIε* acts positively in Fz/PCP signaling.

(A and B) Removal of a copy of *dco* suppresses the *sevFz* phenotype. (A) *sevFz*/+ (at 25ºC). (B) *sevFz*/+, $dco^{dbt\text{-}P}$/+ (25ºC).

(C and D) Removal of a copy of *dco* enhances the *sevStbm* phenotype. (C) *sevStbm*/+ (at 25ºC). (D) *sevStbm*/+, $dco^{dbt\text{-}P}$/+ (25ºC). Because Stbm antagonizes Fz-Dsh function, the enhancement of *sevStbm* by *dco/CKIε* dosage reduction is indicative of a positive requirement in Fz-Dsh signaling.

(E–H) *dco/CKIε* acts positively with *dsh* for both pathways.

(E and F) Removal of a copy of *dco* suppresses the *sev*>Dsh Wg-signaling-related loss-of-photoreceptor phenotype. (E) *sevDsh*/+ (at 29ºC). (F) *sevDsh*/+, $dco^{dbt\text{-}P}$/+ (29ºC). PCP defects are not quantifiable in these backgrounds, because they are masked by the Wg-signaling-related loss of photoreceptors.

(G and H) Removal of a copy of *dsh* suppresses the *sev>CKIε* PCP phenotype. (G) *sev>CKIε*/+ (at 29ºC). (H) *sev>CKIε*/+, dsh^{V26}/+ (29ºC), which is suppressed to a (near) wild-type phenotype. All panels show sections of dorsal areas, except (H), which shows an equatorial region highlighting the good suppression and wild-type equator.

is in a short region of Dsh that is important for Dsh phosphorylation, activity, and signal specificity [18, 19].

Kinase-Dependent and -Independent Functions of CKIε In Vivo

Because previous studies have suggested that CKIε kinase activity is required for its ability to transduce Wnt/β-catenin signals [1, 14], we tested a kinase-dead isoform of CKIε, Dco/CKIεD132N (which affects the ATP binding site; [14, 20]) in vivo. This mutant was unable to transduce Wg signals, but, surprisingly, it induced strong GOF PCP phenotypes in both the eye and wing. *sev*>CKIεD132N eyes display clean PCP phenotypes (Figure 1J; strikingly, PCP defects are cleaner and stronger than *wt* CKIε; compare to Figure 1I). Wings from *dpp*>CKIεD132N flies also display PCP defects, with wing hairs that point away from the expression domain, demonstrating a GOF Fz/PCP phenotype (Figure 4E; compare to *dpp*>Fz and *dpp*>CKIε wings, Figures 2B and 2D).

To investigate the potential for a kinase-independent role of Dco/CKIε, we coexpressed Fz and CKIεD132N (with *dppGAL4*). In contrast to coexpression of Fz and wild-type CKIε (Figure 2C), CKIεD132N did not display extra margin bristles (Figure 4F; Table S1), indicating that kinase activity is important for Wg signaling. Similarly, in contrast to coexpression of Fz2 and wild-type CKIε, *dpp*>Fz2, CKIεD132N (at 18ºC) did not cause an increase in margin bristles as compared to *dpp*>Fz2 alone (Figure 4G, compare to Figure 2F; Table S1). At 25ºC, *dpp*>Fz2, CKIεD132N was not lethal, as compared to *dpp*>Fz2 together wild-type CKIε (Table S1).

In summary, these data demonstrate a requirement for the Dco/CKIε kinase activity in Wg signaling, with CKIεD132N often acting as a dominant negative (Figures S1D and S1E, Table S1, and data not shown), but suggest that kinase activity is not required for Dco/CKIε activity during Fz/PCP signaling.

We next examined the CKIε requirement for Dsh phosphorylation. In an unbiased *Drosophila* S2-cell-based

Table 1. Quantification of genetic interactions with *dco/CKIε* in the Drosophila eye

Genotype	Ommatidial Phenotype (%)			p Value	
	Wild-Type	PCP Defects	Unscorable		
sevFz, +/+ (25C)	62.3 ± 8.1	37.7 ± 8.1	0	0.022	for PCP
sevFz, dco^{dbtP}/+ (25C)	82.2 ± 5.1	17.8 ± 5.1	0		
sevStbm/+ (25C)	87.8 ± 0.9	12.2 ± 0.9	0	0.001	for PCP
sevStbm, dco^{dbtP}/+ (25C)	79.2 ± 2.7	20.8 ± 2.7	0		
sevGal4>UAS-Dsh/+ (29C)	54.3 ± 2.6	16.8 ± 3.2	28.9 ± 2.07	6.44E-05	for scorability
sevGal4>UAS-Dsh, dco^{dbtP}/+ (29C)	77.1 ± 7.1	19.7 ± 7.7	3.19 ± 1.51		
sevGal4>UAS-CKIε/+ (29C)	93 ± 3.5	3.9 ± 1.5	3.1 ± 2.31	0.023	for PCP
dsh^{V26}/+; sevGal4>UAS-CKIε/+ (29C)	97.9 ± 2.3	0.3 ± 0.6	1.71 ± 2.50		
sevGal4>UAS-CKIεD132N/+ (29C)	94.1 ± 2.2	5.6 ± 1.8	0.33 ± 0.57	0.007	for PCP
sevGal4>UAS-CKIεD132N/dco^{dbtP} (29C)	96.2 ± 3.6	1.5 ± 1.1	2.17 ± 4.82		

For each genotype, at least four independent eyes were analyzed. All interactions shown are statistically significant as indicated by the p values. Note that the PCP phenotype of *sevGal4>UASCKIεD132N* is suppressed by the dosage reduction of *dco/CKIε*, whereas the *sevGal4>UASCKIεD132N*-associated "unscorable" phenotype (which reflects other CKIε functions) is enhanced. This suggests that the kinase-dead CKIε isform acts as a gain of function for PCP, whereas it behaves like a mild dominant negative in the other contexts, supporting the notion that CKIε functions independently of its kinase activity in PCP.

screen for kinases that are required for the PCP-signaling-associated Dsh phosphorylation ([21]; A.J., unpublished data), we identified *dco*/CKIε as a kinase required in this context (Figure 4H, compare to the loss of the "upshift" in the PCP-specific Dsh^{1} mutant, Figure 4I). Strikingly, the kinase-dead CKIε isoform, CKIεD132N, promotes PCP-signaling-associated Dsh phosphorylation as much as wild-type CKIε (Figure 4J). These data suggest that although the presence of CKIε protein is important for this phosphorylation event, its kinase activity is not required, consistent with our in vivo expression data with Dco/CKIεD132N.

A possible caveat to these data is that, rather than acting on downstream targets in a kinase-independent manner, CKIεD132N could act to titrate away factors that inhibit the endogenous CKIε. To test this, we examined the effect of CKIεD132N on the phosphorylation of Dsh in S2 cells in the absence of endogenous CKIε. These data show that endogenous CKIε is not mediating the CKIεD132N effect (Figure S2), and thus CKIε is likely to act in a kinase-independent manner in the PCP context.

Conclusions

Our in vivo data support a positive requirement of *dco*/CKIε for peak levels of Wnt/β-catenin signaling and a strict requirement in the Fz/PCP pathway. Whereas the kinase activity of CKIε is required for Wnt/β-catenin signaling, our analysis suggests that it is not required for Fz/PCP signaling. These findings differ from the proposed inhibitory effect of CKIε on Fz/PCP signaling in cell culture [1]. It is possible that the PCP readout in cell culture, namely activation of JNK, only reflects a subset of PCP activities of Dsh, not representing an accurate measure of overall PCP activity. Alternatively, CKIε could act as a constitutively active kinase when expressed in cell culture [22], whereas its activity is regulated in vivo. Thus, for Fz/PCP signaling in vivo, the primary role for CKIε may not be as an active kinase, but rather as a stabilizer of a complex that allows for PCP-specific Dsh phosphorylation. This is supported by our data that the kinase activity of CKIε is not required for Fz/PCP signaling and that kinase-dead CKIε still stimulates phosphorylation of Dsh.

We also demonstrate that CKIε phosphorylates a specific residue in Dsh, S236, in a short region known to be phosphorylated by multiple kinases and suggested to be important in the regulation of Dsh signal specificity [18, 19]. This supports the proposed possibility of in vivo competitive phosphorylation as a mechanism for Dsh regulation. The region upstream of the PDZ domain appears to act as a docking site for Dsh binding proteins. Differential phosphorylation of this region could alter the binding properties of Dsh. In support of this possibility, protein-protein interaction studies have identified a large number of proteins that bind to the Dsh PDZ domain [23]. It is unlikely that all these interactions occur at the same time (e.g., [24]), and phosphorylation is a potential mechanism to regulate this. Further experiments are needed to finely map the many potential phosphorylation target residues and the corresponding kinases and demonstrate their in vivo significance.

Experimental Procedures

Fly Strains and Genetics

Mutant alleles were as follows: *w^{1118}*; *dbt^{P}* (also referred to as *dco* null in this paper; [25]) and *dbt^{AR}* [26] (both gifts from J. Blau); and *dsh^{v26}*. FRT82B, *dbt^{P}* clones were generated by the Flp/FRT technique with *hs*Flp or *ubx*Flp [27] and, in specified instances, by using the *Minute* technique [28], which gives mutant cells of interest a growth advantage. Wing clones were marked by the *forked* mutation. Transgenic flies were generated by standard P element-mediated transformation.

Genetic interactions were tested in the eye by using either *sev*Fz [29] or the Gal4/UAS system [8] with *sev*Gal4 (gift from K.Basler) driving UAS-Stbm [30], UAS-Dsh [31], or UAS-CKIε. For experiments using UAS-Stbm and UAS-CKIε, PCP defects scored were chirality flips and symmetrical clusters. For experiments using *sev*Fz and *sev*Dsh, PCP defects scored were only symmetrical clusters, because the loss of an equator makes scoring for chirality flips difficult. For all experiments, unscorable ommatidia were identified as those with an incorrect complement of photoreceptors.

For PCP analysis and coexpression in the wing, we used *dpp*Gal4 driving UAS-Fz1-1-1, UAS-Fz2-2-2 [31], UAS-CKIε, and/or UAS-CKIεD132N.

Histology and Immunohistochemistry

Tangential sections of adult eyes were prepared as described [29]. Wings were incubated in PBS + 0.1% Triton X-100 overnight, mounted in 80% glycerol [31], and viewed on a Zeiss Axioplan microscope. Stainings of imaginal discs were performed as described [32], mounted in Vectashield (Vector Labs), and scanned on a Zeiss confocal microscope. Single optical sections were analyzed with the

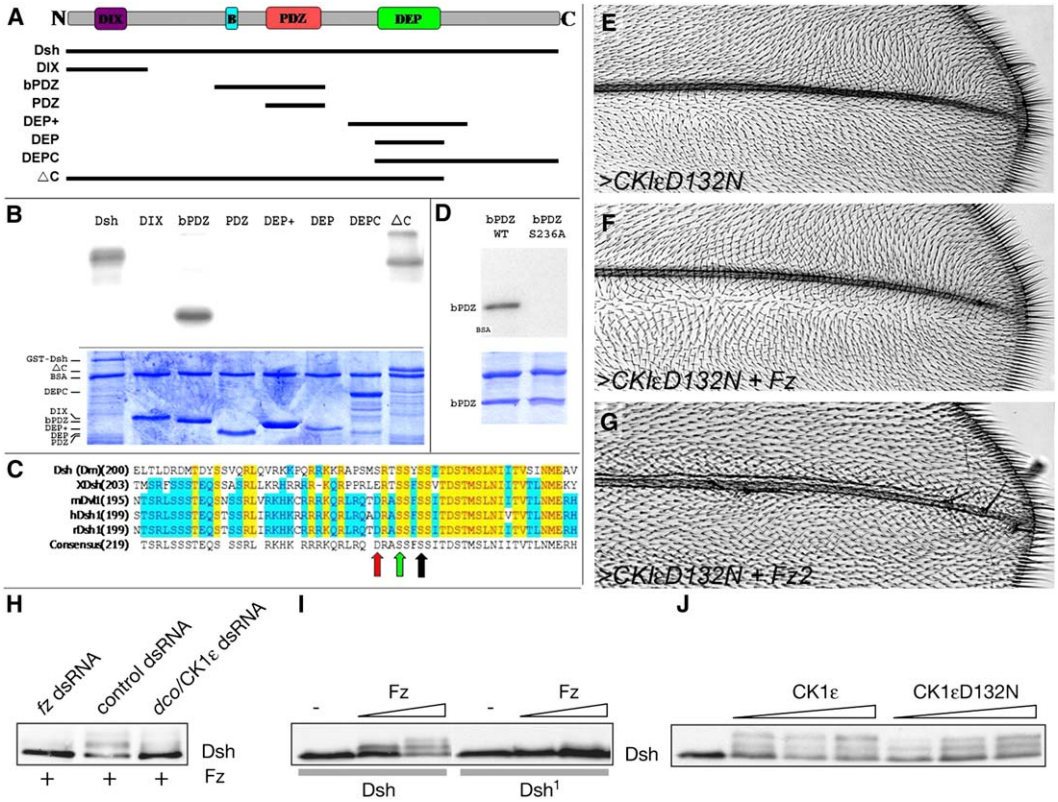

Figure 4. Kinase-Dependent and -Independent Functions of CKIε

(A) Schematic representation of Dsh with the respective GST-Dsh constructs used below for in vitro kinase assays. Full-length Dsh contains the conserved DIX domain, basic region, PDZ domain, and DEP domain as highlighted. All constructs were made and purified as N-terminal GST fusion proteins.

(B) Autoradiograph of an in vitro kinase assay with recombinant, purified CKIε and the GST-Dsh constructs diagrammed in (A). The GST constructs are indicated on the top of each lane. Sizes of the corresponding GST fusion proteins are marked on the left. (B′) shows a Coomassie stain of the gel from (B), indicating equal loading of all GST-Dsh constructs.

(C) Alignment of the amino acids contained in the bPDZ construct N terminal to the PDZ domain. The arrows below the alignment indicate amino acids predicted to be part of a CKIε consensus motif. The red arrow indicates S233, and the green arrow indicates S236.

(D) Autoradiograph of an in vitro kinase assay with recombinant, purified CKIε and either GST-bPDZ or GST-bPDZS236A. The GST constructs are indicated on the top of each lane, and their migration is marked on the left. (D′) shows a Coomassie stain of the gel from (D), indicating equal loading of both GST-bPDZ constructs.

(E–G) Kinase-dead CKIε promotes PCP signaling in the wing, but does not synergize with Fz or Fz2 for Wg signaling. (E) *dpp*Gal4>UAS-CKIεD132N wing (at 25ºC). Wing hairs point away from the *dpp* stripe, indicating a GOF PCP phenotype. (F) *dpp*Gal4>UAS-CKIεD132N, UAS-Fz wing (at 25ºC). Note lack of extra margin bristles compared with Figure 2C. (G) *dpp*Gal4>UAS-CKIεD132N, UAS-Fz2 wing (at 18ºC). Note the lack of extra margin bristles compared with Figure 2E.

(H–J) CKIε promotes the PCP-specific phosphorylation of Dsh in a kinase-independent manner. Western blots show anti-Myc staining, detecting Dsh. (H) *dco*/CKIε is required for the Fz-induced band shift of Dsh. S2 cells were cotransfected with Fz and Dsh and treated with the indicated dsRNAs. Note that CKIε-dsRNA abrogates Dsh phosphorylation as well as dsRNA against Fz. (I) A PCP-specific mutation of Dsh in the DEP domain prevents its Fz-induced band shift in S2 cells, consistent with in vivo data [21]. S2 cells were cotransfected with either wild-type Dsh (left) or DshK417M (Dsh^1; right) and increasing amounts of Fz. (J) The kinase activity of CKIε is not required to induce phosphorylation band shift of Dsh. S2 cells were cotransfected with Dsh and increasing amounts of CKIε or CKIεD132N as indicated. See Experimental Procedures for details.

Zeiss LSM 5 Image Browser and Adobe Photoshop software. The following primary antibodies were used: Guinea Pig anti-Sens (gift from H. Bellen; 1:1000), mouse anti-myc (Santa Cruz Biotech; 1:250), mouse anti-Wg (1:5), anti-Dll (1:200; both from S. Cohen), rabbit anti-βGal (Cappel; 1:1000), and mouse anti-Caspase3 (Molecular Probes).

Molecular Biology and Biochemistry

Dco/CKIε DNA was cloned by PCR as an EcoRI-XhoI fragment from a third-larval-instar cDNA library (ATCC #87290). CKIεD132N was generated by site-directed mutagenesis (Quickchange/Stratagene). All PCR products were sequenced in their entirety.

For in vitro kinase assays, all GST fusion proteins used were previously described [24]. Kinase assays were performed with purified human CKIε (Invitrogen) and the GST proteins described. Samples of 20 μl containing 2 μg GST protein, 500 pg CKIε, 0.5 μl $\gamma^{[32]}$P ATP (Amersham PB10168; 10 mCi/ml, ~3000 Ci/mmol) in kinase buffer (75 μM ATP, 0.5 mM DTT, 7 mM MgCl2, 100 μg/ml BSA, 30 mM HEPES [pH 7.5]) were incubated for 30 min at 37ºC and subjected to SDS-PAGE electrophoresis. Gels were stained with Coomasie solution to reveal protein content, dried, and subjected to autoradiography.

For shift assays in S2 cells, Fz, Myc5-DshMyc, Myc5Dsh^1Myc, and CK1ε were cloned into pAc5.1 (Invitrogen). For RNAi experiments, S2 cells were batch transfected with pAcFz and pAcMyc5DshMyc. Fifty thousand cells were replated into 96-well plates after 1 day and fed with 1 μg of the indicated dsRNA for 4 more days. For the shifts in Figure 4I, 200 ng of pAcMyc5DshMyc and Myc5Dsh^1Myc were transfected alone and together with 10 and 50 ng pAcFz in 12-well plates. For the shift of Dsh by CK1ε, 100 ng of pAcMyc5DshMyc was transfected alone and together with 100, 250, and 500 ng of CK1ε or CK1εD132N. Empty pAc5.1 was used to fill up transfections.

Two days after transfection, cells were lysed and samples were run on 12% Anderson gels [33], transferred to PVDF, and probed with anti-Myc antibody (1:1000; Santa Cruz).

Supplemental Data

Supplemental Data include one table and two figures and are available with this article online at: http://www.current-biology.com/cgi/content/full/16/13/1337/DC1/.

Acknowledgments

We are grateful to J. Blau for fly strains and insightful conversation, K Bartscherer and M. Boutros for sharing unpublished results, H. Bellen and S. Cohen for antibodies, and K. Basler and the Bloomington Stock Center for fly strains. We thank M. Nugent, S. Okello, and S. Schreier for technical help. Confocal laser microscopy was performed at the MSSM-Microscopy SRF, supported by a National Institutes of Health (NIH)/National Cancer Institute shared instrumentation grant. We thank J. Bieker and all members of the Mlodzik lab for helpful discussions, technical advice, and critical readings of the manuscript. This research was supported by NIH/National Eye Institute grant RO1 EY13256 to M.M.

Received: March 15, 2006
Revised: June 2, 2006
Accepted: June 9, 2006
Published: July 10, 2006

References

1. Cong, F., Schweizer, L., and Varmus, H. (2004). Casein kinase Iepsilon modulates the signaling specificities of dishevelled. Mol. Cell. Biol. *24*, 2000–2011.
2. Zilian, O., Frei, E., Burke, R., Brentrup, D., Gutjahr, T., Bryant, P.J., and Noll, M. (1999). double-time is identical to discs overgrown, which is required for cell survival, proliferation and growth arrest in Drosophila imaginal discs. Development *126*, 5409–5420.
3. Bartscherer, K., Pelte, N., Ingelfinger, D., and Boutros, M. (2006). Secretion of Wnt ligands requires Evi, a conserved transmembrane protein. Cell *125*, 523–533.
4. Mlodzik, M. (1999). Planar polarity in the *Drosophila* eye: A multifaceted view of signaling specificity and cross-talk. EMBO J. *18*, 6873–6879.
5. Strutt, H., and Strutt, D. (1999). Polarity determination in the Drosophila eye. Curr. Opin. Genet. Dev. *9*, 442–446.
6. Adler, P.N. (2002). Planar signaling and morphogenesis in Drosophila. Dev. Cell *2*, 525–535.
7. Swiatek, W., Tsai, I.C., Klimowski, L., Pepler, A., Barnette, J., Yost, H.J., and Virshup, D.M. (2004). Regulation of casein kinase I epsilon activity by Wnt signaling. J. Biol. Chem. *279*, 13011–13017.
8. Brand, A.H., and Perrimon, N. (1993). Targeted gene expression as a means of altering cell fates and generating dominant phenotypes. Development *118*, 401–415.
9. Adler, P.N., Taylor, J., and Charlton, J. (2000). The domineering non-autonomy of frizzled and van Gogh clones in the Drosophila wing is a consequence of a disruption in local signaling. Mech. Dev. *96*, 197–207.
10. Taylor, J., Abramova, N., Charlton, J., and Adler, P.N. (1998). Van Gogh: A new Drosophila tissue polarity gene. Genetics *150*, 199–210.
11. Wolff, T., and Rubin, G.M. (1998). *strabismus*, a novel gene that regulates tissue polarity and cell fate decisions in *Drosophila*. Development *125*, 1149–1159.
12. Brunner, E., Peter, O., Schweizer, L., and Basler, K. (1997). pangolin encodes a Lef-1 homologue that acts downstream of Armadillo to transduce the Wingless signal in Drosophila. Nature *385*, 829–833.
13. Gao, Z.H., Seeling, J.M., Hill, V., Yochum, A., and Virshup, D.M. (2002). Casein kinase I phosphorylates and destabilizes the beta-catenin degradation complex. Proc. Natl. Acad. Sci. USA *99*, 1182–1187.
14. Peters, J.M., McKay, R.M., McKay, J.P., and Graff, J.M. (1999). Casein kinase I transduces Wnt signals. Nature *401*, 345–350.
15. Sakanaka, C., Leong, P., Xu, L., Harrison, S.D., and Williams, L.T. (1999). Casein kinase iepsilon in the wnt pathway: Regulation of beta-catenin function. Proc. Natl. Acad. Sci. USA *96*, 12548–12552.
16. Flotow, H., Graves, P.R., Wang, A.Q., Fiol, C.J., Roeske, R.W., and Roach, P.J. (1990). Phosphate groups as substrate determinants for casein kinase I action. J. Biol. Chem. *265*, 14264–14269.
17. Meggio, F., Perich, J.W., Marin, O., and Pinna, L.A. (1992). The comparative efficiencies of the Ser(P)-, Thr(P)- and Tyr(P)-residues as specificity determinants for casein kinase-1. Biochem. Biophys. Res. Commun. *182*, 1460–1465.
18. Ossipova, O., Dhawan, S., Sokol, S., and Green, J.B. (2005). Distinct PAR-1 proteins function in different branches of Wnt signaling during vertebrate development. Dev. Cell *8*, 829–841.
19. Penton, A., Wodarz, A., and Nusse, R. (2002). A mutational analysis of dishevelled in Drosophila defines novel domains in the dishevelled protein as well as novel suppressing alleles of axin. Genetics *161*, 747–762.
20. Zhu, J., Shibasaki, F., Price, R., Guillemot, J.C., Yano, T., Dotsch, V., Wagner, G., Ferrara, P., and McKeon, F. (1998). Intramolecular masking of nuclear import signal on NF-AT4 by casein kinase I and MEKK1. Cell *93*, 851–861.
21. Axelrod, J.D., Miller, J.R., Shulman, J.M., Moon, R.T., and Perrimon, N. (1998). Differential requirement of Dishevelled provides signaling specificity in the Wingless and planar cell polarity signaling pathways. Genes Dev. *12*, 2610–2622.
22. Cegielska, A., Gietzen, K.F., Rivers, A., and Virshup, D.M. (1998). Autoinhibition of casein kinase I epsilon (CKI epsilon) is relieved by protein phosphatases and limited proteolysis. J. Biol. Chem. *273*, 1357–1364.
23. Wallingford, J.B., and Habas, R. (2005). The developmental biology of Dishevelled: An enigmatic protein governing cell fate and cell polarity. Development *132*, 4421–4436.
24. Jenny, A., Reynolds-Kenneally, J., Das, G., Burnett, M., and Mlodzik, M. (2005). Diego and Prickle regulate Frizzled planar cell polarity signalling by competing for Dishevelled binding. Nat. Cell Biol. *7*, 691–697.
25. Kloss, B., Price, J.L., Saez, L., Blau, J., Rothenfluh, A., Wesley, C.S., and Young, M.W. (1998). The Drosophila clock gene double-time encodes a protein closely related to human casein kinase Iepsilon. Cell *94*, 97–107.
26. Rothenfluh, A., Abodeely, M., and Young, M.W. (2000). Short-period mutations of per affect a double-time-dependent step in the Drosophila circadian clock. Curr. Biol. *10*, 1399–1402.
27. Xu, T., and Rubin, G.M. (1993). Analysis of genetic mosaics in developing and adult *Drosophila* tissues. Development *117*, 1223–1237.
28. Garcia-Bellido, A., Ripoll, P., and Morata, G. (1976). Developmental compartmentalization in the dorsal mesothoracic disc of Drosophila. Dev. Biol. *48*, 132–147.
29. Boutros, M., Paricio, N., Strutt, D.I., and Mlodzik, M. (1998). Dishevelled activates JNK and discriminates between JNK pathways in planar polarity and *wingless* signaling. Cell *94*, 109–118.
30. Rawls, A.S., and Wolff, T. (2003). Strabismus requires Flamingo and Prickle function to regulate tissue polarity in the Drosophila eye. Development *130*, 1877–1887.
31. Wu, J., Klein, T.J., and Mlodzik, M. (2004). Subcellular localization of frizzled receptors, mediated by their cytoplasmic tails, regulates signaling pathway specificity. PLoS Biol. *2*, 1004–1014.
32. Weber, U., Paricio, N., and Mlodzik, M. (2000). Jun mediates Frizzled induced R3/R4 cell fate distinction and planar polarity determination in the *Drosophila* eye. Development *127*, 3619–3629.
33. Riechmann, V., and Ephrussi, A. (2004). Par-1 regulates bicoid mRNA localisation by phosphorylating Exuperantia. Development *131*, 5897–5907.